Cellular/Molecular

Accumulation of Laminin Monomers in *Drosophila* Glia Leads to Glial Endoplasmic Reticulum Stress and Disrupted Larval Locomotion

Lindsay M. Petley-Ragan,[1,3] Evan L. Ardiel,[2] Catharine H. Rankin,[2] and Vanessa J. Auld[1,3]

Departments of [1]Zoology and [2]Psychology, University of British Columbia, Vancouver, British Columbia V6T 1Z4, Canada, and [3]Neuroscience Research Group, Life Sciences Institute, University of British Columbia, Vancouver, British Columbia V6T 1Z3, Canada

The nervous system is surrounded by an extracellular matrix composed of large glycoproteins, including perlecan, collagens, and laminins. Glial cells in many organisms secrete laminin, a large heterotrimeric protein consisting of an α, β, and γ subunit. Prior studies have found that loss of laminin subunits from vertebrate Schwann cells causes loss of myelination and neuropathies, results attributed to loss of laminin-receptor signaling. We demonstrate that loss of the laminin γ subunit (LanB2) in the peripheral glia of *Drosophila melanogaster* results in the disruption of glial morphology due to disruption of laminin secretion. Specifically, knockdown of LanB2 in peripheral glia results in accumulation of the β subunit (LanB1), leading to distended endoplasmic reticulum (ER), ER stress, and glial swelling. The physiological consequences of disruption of laminin secretion in glia included decreased larval locomotion and ultimately lethality. Loss of the γ subunit from wrapping glia resulted in a disruption in the glial ensheathment of axons but surprisingly did not affect animal locomotion. We found that Tango1, a protein thought to exclusively mediate collagen secretion, is also important for laminin secretion in glia via a collagen-independent mechanism. However loss of secretion of the laminin trimer does not disrupt animal locomotion. Rather, it is the loss of one subunit that leads to deleterious consequences through the accumulation of the remaining subunits.

Key words: *Drosophila*; ER stress; glia; laminin; neuropathy; Tango1

Significance Statement

This research presents a new perspective on how mutations in the extracellular matrix protein laminin cause severe consequences in glial wrapping and function. Glial-specific loss of the β or γ laminin subunit disrupted glia morphology and led to ER expansion and stress due to retention of other subunits. The retention of the unpaired laminin subunit was key to the glial disruption as loss of Tango1 blocked secretion of the complete laminin trimer but did not lead to glial or locomotion defects. The effects were observed in the perineurial glia that envelope the peripheral and central nervous systems, providing evidence for the importance of this class of glia in supporting nervous system function.

Introduction

Basement membranes are composed of large glycoproteins that form an extracellular matrix (ECM) around organs to provide them with structural and functional support. Laminin, a conserved component of basement membranes, is a heterotrimer composed of an α, β, and γ subunit. Vertebrates have multiple genes for all three laminin subunits, resulting in 18 different laminin isoforms. Mutations in individual laminin subunits can cause hereditary diseases, including congenital muscular dystrophy type IA [Online Mendelian Inheritance in Man (OMIM) #607855], characterized by peripheral dysmyelination and brain defects, and Pierson syndrome (OMIM #609049), characterized by renal failure, vision loss, and muscular and neurological defects (Feltri and Wrabetz, 2005; Durbeej, 2010). Laminin is essen-

Received May 3, 2015; revised Oct. 30, 2015; accepted Dec. 9, 2015.

Author contributions: L.M.P.-R. and V.J.A. designed research; L.M.P.-R. performed research; E.L.A. and C.H.R. contributed unpublished reagents/analytic tools; L.M.P.-R. and V.J.A. analyzed data; L.M.P.-R. and V.J.A. wrote the paper.

This work was supported by grants to C.H.R. [Canadian Institutes of Health Research (CIHR) MOP-130287; Natural Sciences and Engineering Research Council of Canada (NSERC) RGPIN 1222216-13] and V.J.A. (CIHR MOP-123420; NSERC RGPIN 2014-04511). L.M.P.-R. was supported by a scholarship from the Multiple Sclerosis Society of Canada. We thank Dr. Cath Cowen for TEM assistance, Drs. Doug Allan and Elizabeth Davis for fly stocks, and Dr. Mary Gilbert for comments on the manuscript.

The authors declare no competing financial interests.

Correspondence should be addressed to Vanessa J. Auld, 2350 Health Sciences Mall, Life Sciences Institute, University of British Columbia, Vancouver, BC V6T 1Z3, Canada. E-mail: auld@zoology.ubc.ca.

DOI:10.1523/JNEUROSCI.1797-15.2016

 0270-6474/16/361151-14$15.00/0

tial in peripheral nervous system (PNS) development for proper sorting and myelination of axons by Schwann cells (Yu et al., 2009a,b). Furthermore, mutants of laminin isoforms in Schwann cells have disrupted Schwann cell radial sorting, myelination, differentiation, and survival (Wallquist et al., 2005; Yang et al., 2005; Yu et al., 2005, 2007). Vertebrate research has focused on a lack of laminin-receptor signaling as the underlying cause of dysmyelination and neurological defects (Feltri et al., 2002; Yu et al., 2007). Studies in other tissues have focused on receptor-independent effects of laminin loss. For example, studies done in kidney found that β laminin mutations triggered endoplasmic reticulum (ER) stress, potentially due to defective secretion of remaining subunits (Chen et al., 2011, 2013). This led us to the hypothesis that disruption to laminin secretion in glia may contribute to the neurological defects associated with laminin mutations.

Laminin trimerization occurs in the ER where the β and γ subunits assemble and require α subunit incorporation to form a functional laminin heterotrimer before secretion (Yurchenco et al., 1997). If either the β or γ subunit is missing, the other accumulates intracellularly and the α subunit is secreted alone (Yurchenco et al., 1997). This model of laminin secretion was supported by studies in *Caenorhabditis elegans* that showed intracellular β laminin accumulation in body-wall muscles and intestine when α laminin was mutated (Huang et al., 2003; Kao et al., 2006). However, neither the physiological and cellular effects of accumulated laminin subunits nor the mechanism of laminin secretion have been determined.

In *Drosophila*, there are 2 α (Wb and LanA), 1 β (LanB1), and 1 γ (LanB2) subunits. Mutations in LanB1 result in embryonic lethality, absent basement membranes, and accumulation of other ECM proteins in mutant tissues (Urbano et al., 2009; Wolfstetter and Holz, 2012). The embryonic lethality of laminin mutations is likely because many tissues secrete laminin during development, including hemocytes and fat bodies, both of which contribute to the ECM surrounding tissues, such as the nervous system (Bunt et al., 2010; Pastor-Pareja and Xu, 2011). Muscle cells also secrete laminin and secretion of LanA regulates larval neuromuscular junction growth (Tsai et al., 2012). In this study we investigated the cellular and physiological consequences of laminin knockdown in the peripheral glia and examined whether changes to the glia led to disruption in animal locomotion and survival.

We found that glial knockdown of the laminin subunits with a focus on the γ subunit LanB2 resulted in glial swelling and accumulation of the remaining β subunit (LanB1) in the ER. The knockdown of LanB2 in all glia and the perineurial glia led to ER stress, decreased larval locomotion, and eventual larval death. Loss of LanB2 in the wrapping glia disrupted axon ensheathment but did not disrupt larval locomotion. Furthermore, we determined that Tango1, a mediator of collagen secretion from the ER (Malhotra and Erlmann, 2011), also mediates laminin secretion via a collagen-independent mechanism. Together, our results, by providing evidence for receptor-independent mechanisms through which a loss of laminin in glia affects glial structure and function, opens a new perspective on the cause of peripheral neuropathies associated with laminin mutations.

Materials and Methods

Fly strains and genetics. The following fly strains used in this study were obtained from the Bloomington Stock Center: *repo-GAL4* (Sepp et al., 2001); *nrv2-GAL4* (Sun et al., 1999); UAS-mCD8::GFP (Lee and Luo, 1999); UAS-Dicer2 (Dietzl et al., 2007); UAS-KDEL::GFP (#9898); UAS-LanB1$^{EP\text{-}600}$ (Molnar et al., 2006); UAS-hid; UAS-rpr; Viking::GFP (Morin et al., 2001); Df(2L)Exel7032L; UAS-CD8::RFP; UAS-GFP. *46F-GAL4* (Xie and Auld, 2011) was obtained from the Kyoto Stock Center. The *xbp1>dsRed* (Ryoo et al., 2013) line was a gift from Dr. Don Ryoo. The RNAi lines from the Vienna *Drosophila* RNAi Centre were as follows: LanA RNAi (GD6022), LanB1 RNAi (GD13179), LanB2 RNAi (GD2394), Tango1 RNAi (GD956). The LanA RNAi line (JF02908) was from the Bloomington Stock Center. All transmission electron microscopic (TEM), confocal, and projection images are of third-instar larvae nerves and experiments were performed at 29°C with UAS-Dicer2. All larval tracking experiments were performed at 25°C with controls expressing UAS-Dicer2 and UAS-mCD8::GFP in glia. Larvae of either sex were used in all experiments.

Immunolabeling and image analysis. Dissection and fixation for immunofluorescence was performed as described previously (Sepp et al., 2000). For immunolabeling, larvae were fixed in 4% formaldehyde for 15–30 min. The following primary antibodies were used: rabbit anti-LanB1 (1:500; Abcam), rabbit anti-LanB2 (1:500; Abcam), rabbit anti-HRP (1:500; Jackson ImmunoResearch). Secondary antibodies were goat anti-mouse or goat anti-rabbit conjugated with Alexa 488, Alexa 568, or Alexa 647 (1:300; Invitrogen).

High-magnification fluorescent images were obtained with a DeltaVision (Applied Precision) using a 60× oil-immersion objective (numerical aperture, 1.4) at 0.2 μm steps. Stacks were deconvolved (SoftWorx) using a measured point spread function using 0.2 μm fluorescent beads (Invitrogen) in Vectashield (Vector Laboratories). Low-magnification images were taken using a 20× water-immersion lens (numerical aperture, 0.95) on a Leica confocal microscope. Images were compiled using Photoshop and Illustrator CS4. For all 60× images, a single *Z* slice is shown. For TEM analysis, larval brains were fixed in 4% formaldehyde and 3% glutaraldehyde, rinsed in 0.1 M PIPES, postfixed in 1% osmium tetroxide, embedded in 1:1 acetonitrile/Spurr resin, and polymerized in Spurr resin. Thin sections (50 nm) were obtained with a Leica ultramicrotome and analyzed with an FEI Tecnai TEM operating at an accelerating voltage of 80 kV.

Larval tracking. Larval tracking was performed using an adapted multiworm tracker and script (Swierczek et al., 2011). Each tracking session included 5–30 larvae placed on 100-mm-diameter apple juice plates, tapped to elicit movement, and tracked for 30 s. The instantaneous speed of all larvae at 15 s was measured and differences analyzed using a one-way ANOVA plus Tukey's *post hoc* test.

Morphological quantification. Nerve diameters in Figure 6 were measured at the widest point along nerves within 300 μm of the exit from the ventral nerve cord and analyzed using a one-way ANOVA and Tukey's *post hoc* test. In Figure 7, nerves with ≥1 section in which no wrapping glial processes were observed using *nrv2>GFP* were defined as discontinuous. Nerves with ≥1 membrane-bound swelling as large as a wrapping glial nucleus were counted as nerves with vacuole-like structures. Unpaired *t* tests were used to calculate *p* values between controls and experimental averages.

Results

Knockdown of laminin subunits in glia results in severe morphological defects and death

To study the role of glial-derived laminin in PNS nerves, we used glial-specific expression of RNAi to knock down individual laminin subunits in *Drosophila* glia and examined the resulting glial morphology and function in larval stages. Since *Drosophila* glia express laminin but neither perlecan nor collagen-IV (Xie and Auld, 2011), the study of laminin secretion is not affected by the secretion of other major ECM proteins from this tissue. The PNS of the *Drosophila* third-instar larva is composed of three distinct glial layers that surround motor and sensory axons (Fig. 1*H*; Stork et al., 2008). The innermost layer, the wrapping glia (Fig. 1*H*, magenta), is similar to nonmyelinating Schwann cells in that it directly contacts and ensheaths axons. The middle layer, the subperineurial glia (Fig. 1*H*, orange), encircles the wrapping

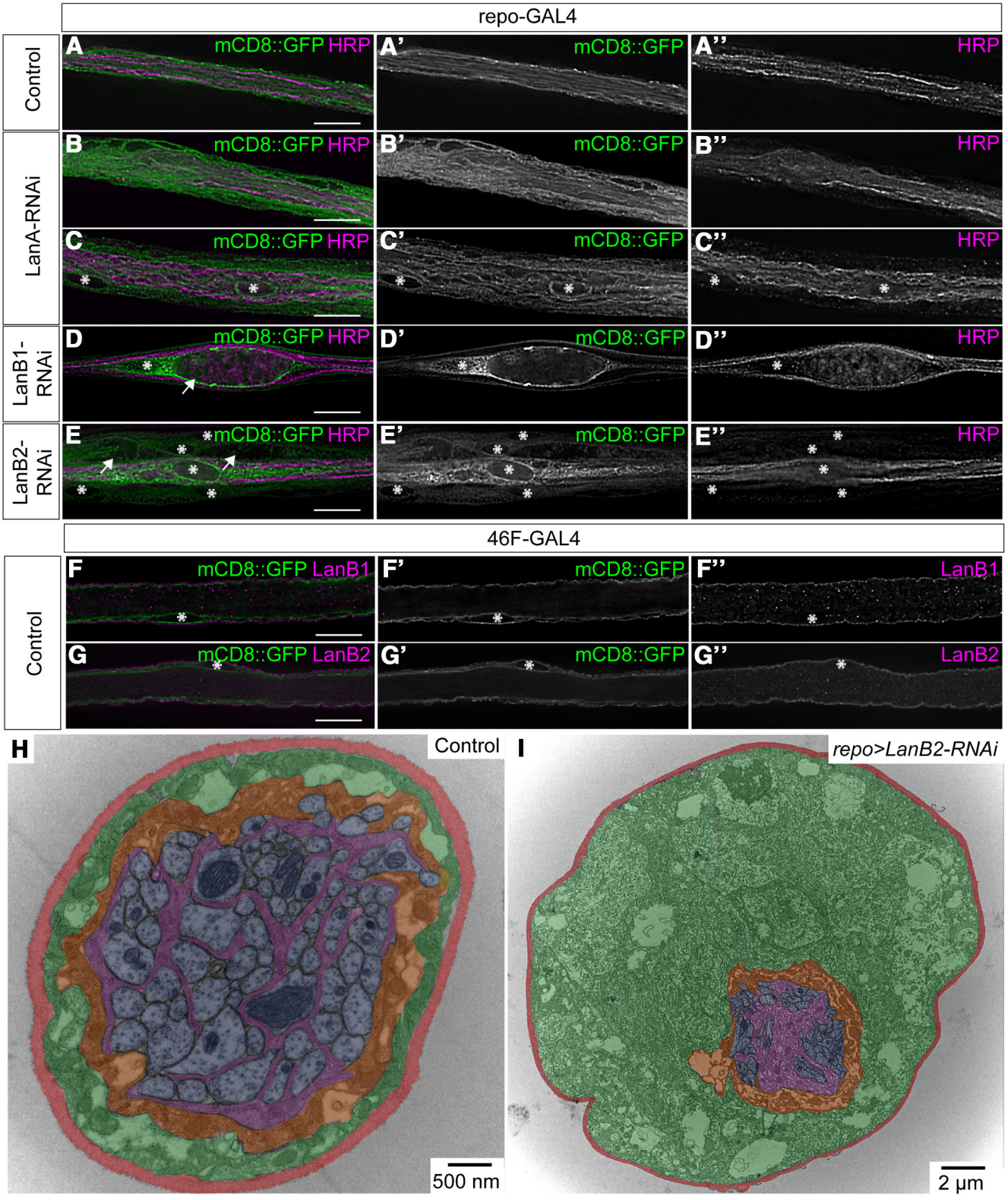

Figure 1. Laminin subunit knockdown results in peripheral glial swelling. ***A–G***, Longitudinal sections of peripheral nerves with glial membranes labeled with mCD8::GFP (green) and axons immunolabeled using anti-HRP antibody (magenta). Asterisks mark nuclei. Scale bars, 15 μm. ***A***, Control peripheral nerve. ***B–E***, RNAi against LanA (***B***, ***C***), LanB1 (***D***), or LanB2 (***E***) resulted in wider nerves and vacuole-like structures (arrows). ***F***, ***G***, Control perineurial glial membranes were labeled with mCD8::GFP (green) and the ECM immunolabeled using anti-LanB2 or anti-LanB1 antibody (magenta). Laminin is found predominantly exterior to the perineurial glia. ***H***, ***I***, TEM images of peripheral nerve sections from control (*repo-GAL4*; ***H***) or *repo>LanB2-RNAi* (***I***) larvae. Panels are false colored to show ECM (red), perineurial glia (green), subperineurial glia (orange), wrapping glia (magenta), and axons (blue). Control nerves have a thin layer of perineurial glia (***H***), while LanB2 knockdown generates severely swollen perineurial glia with vacuole-like structures (***I***). Scale bars: ***H***, 0.5 μm; ***I***, 2 μm.

Table 1. Summary of survival and mobility of genotypes

Genotype	Mobility	Lethality
repo-GAL4	++	Viable
repo>LanB2-RNAi	−	Lethal (third instar)
repo>Tango1-RNAi	++	Lethal (pupal)
repo>LanB2-RNAi, Df(LanB1)	−	Lethal (third instar)
repo>LanB1	++	Viable
46F-GAL4	++	Viable
46F>LanB2-RNAi	+	Lethal (pupal)
46F>Tango1-RNAi	++	Viable
46F>hid,rpr	−*	Lethal (early larval)
nrv2-GAL4	++	Viable
nrv2>LanB2-RNAi	++	Viable
nrv2>hid,rpr	−	Lethal (pupal)

++, Average speed not significantly different than controls; +, average speed significantly slower than controls; −, average speed less than 1.5 mm/s.

*GAL80ts present and temperature shifted to 29°C for 24 h; third-instar larvae were immobile.

glia and forms the blood–brain barrier via septate junctions. The outermost layer, the perineurial glia (Fig. 1*H*, green), is surrounded by a basement membrane composed of an extensive ECM, or neural lamella (Fig. 1*H*, red). While the overlying ECM contains perlecan, laminin, and collagen IV, glia do not secrete perlecan or collagen IV (Stork et al., 2008; Xie and Auld, 2011). To test whether the perineurial glia were contributing laminin to the ECM, we used GAL4 drivers to express membrane-tagged fluorescent markers (mCD8::GFP) in the perineurial glia (*46F-GAL4*) and assayed for the presence of laminin subunits in peripheral nerves. Immunolabeling confirmed the presence of the β subunit, LanB1, and the γ subunit, LanB2, in the ECM surrounding the perineurial glia (Fig. 1*F*,*G*). This is similar to vertebrates where axon fascicles of peripheral nerves are surrounded by a layer of ECM containing collagen, nidogen, perlecan, and laminin (Yurchenco, 2011).

To test the role of laminin in the peripheral glia, we used RNAi transgenes to knock down laminin expression in all glia using *repo-GAL4*. Unfortunately, quantification of laminin deposition in the neural lamella by glia is not possible as hemocytes and fat bodies contribute extensively to the ECM surrounding peripheral nerves (Bunt et al., 2010; Pastor-Pareja and Xu, 2011). To overcome this limitation, we used a range of RNAi lines to knock down the α subunit, LanA, or the LanB1 and LanB2 subunits. We used two LanA RNAi lines, one of which (GD6022) has been previously used (Tsai et al., 2012), and individual LanB1 and LanB2 lines. All larvae analyzed demonstrated a peripheral nerve phenotype (LanA RNAi, $n = 25$; LanB1 RNAi, $n = 30$; LanB2 RNAi, $n = 75$). The peripheral nerve phenotypes resulting from knockdown of LanA included wider peripheral nerves characterized by glial swelling and small vacuoles (Fig. 1*B*,*C*). In all larvae analyzed, knockdown of LanB1 or LanB2 also resulted in peripheral nerve phenotypes that were similar but stronger and consisted of severe glial swelling and large vacuoles in addition to larval death (Fig. 1*D*,*E*; Table 1). None of the RNAi constructs significantly affected axon morphology at this resolution (Fig. 1*A*″–*E*″). Swollen areas or vacuoles were never observed in control larvae (*repo-GAL4* with *UAS-Dicer2* and *UAS-mCD8::GFP*, $n = 170$). Similar observations with four different RNAi constructs against three separate laminin subunits suggest that the phenotypes are unlikely due to off-target effects of the RNAi constructs. The most penetrant phenotype was seen with LanB2-RNAi, and we used this line for all subsequent experiments. To further characterize the ultrastructure of the swollen nerves, we analyzed peripheral nerves of control and *repo>LanB2-RNAi* larvae using TEM (Fig. 1*H*,*I*). All LanB2-RNAi larvae ($n = 8$) had peripheral nerve glia with large vacuoles, extensive ER, and increased width, phenotypes not observed in any control larvae ($n = 12$). The majority of the swelling was due to the increased size of the perineurial glia, which contained multiple vacuole-like structures (Fig. 1*I*). Note the scale difference between control (500 nm) and LanB2 knockdown (2 μm) due to the increased diameter and size of the outermost layer of perineurial glia.

We found that expression of LanB2 RNAi using the perineurial glia driver *46F-GAL4* also resulted in glial swelling and vacuoles (Fig. 2*F*,*G*). The phenotypes were observed in all larvae ($n = 80$) compared with controls, where this phenotype was never observed ($n = 80$). LanB1 RNAi was expressed in the perineurial glia using *46F-GAL4* and showed a similar phenotype to *46F>LanB2-RNAi* but with a lower penetrance (Fig. 2*H*). Though we observed more severe phenotypes using *repo-GAL4* than *46F-GAL4* (Fig. 2*C*,*D*), the knockdown of LanB2 was lethal using both drivers, with lethality occurring in late third-instar larval stages and pupae respectively (Table 1). It is possible that glial layers other than the perineurial glia contribute to the more severe phenotypes seen using *repo-GAL4* or that *repo-GAL4* is stronger and expressed earlier. Overall these results demonstrate that glial cells, and specifically perineurial glial cells, express laminin and that glia are severely affected when LanB2 is knocked down.

LanB2 knockdown results in intracellular accumulation of LanB1

In vitro studies have shown that the absence of either the β or γ subunit prevents their dimerization and results in the intracellular accumulation of the unpaired monomeric subunit while the α subunit is secreted alone (Yurchenco et al., 1997). We hypothesized that the swollen areas of the glia when LanB2 is knocked down may contain accumulated LanB1 protein. Expression of LanB2 RNAi using either *repo-GAL4* or *46F-GAL4* resulted in large accumulations of LanB1 within the interior of the peripheral glia (Fig. 2*C*,*D*,*F*,*G*). Similarly, expression of LanB1 RNAi with *46F-GAL4* led to accumulation of LanB2 within the peripheral glia (Fig. 2*H*). Accumulations were found in concentrated GFP-labeled deposits (Fig. 2*D*,*F*), as well as clustered puncta within the cytosol (Fig. 2*G*,*H*). Accumulations were observed in all LanB2-RNAi larvae ($n = 35$) but never observed in controls ($n = 35$). Rather, controls displayed the normal concentration of LanB1 along the exterior of the nerve within the neural lamella (Fig. 2*B*,*E*). LanB1 accumulations were observed in glia within both the CNS and PNS and coincided with the swollen regions in the peripheral nerves (Fig. 2*C*).

LanB2 knockdown results in increased ER and ER stress

A prediction of the laminin secretion model from *in vitro* studies is that LanB1 accumulations are likely to be primarily unbound LanB1 monomers (Yurchenco et al., 1997), which in turn may lead to changes to the ER. Our ultrastructural analysis found that knockdown of LanB2 in *Drosophila* glia resulted in areas of increased ribosomes and expanded ER in many nerves (Fig. 3*B*,*B*″). To determine whether the accumulated LanB1 was localized to the expanded ER, we coexpressed LanB2 RNAi and a GFP-tagged ER marker, KDEL::GFP, in perineurial glia and then immunolabeled for LanB1. In control larvae ($n = 15$), KDEL::GFP was evenly distributed throughout perineurial glia and LanB1 was found in the ECM (Fig. 3*C*). After LanB2 knockdown, we observed GFP-positive aggregates in the CNS and PNS that colocalized with LanB1 in all mutant larvae ($n = 10$; Fig. 3*D*). The size

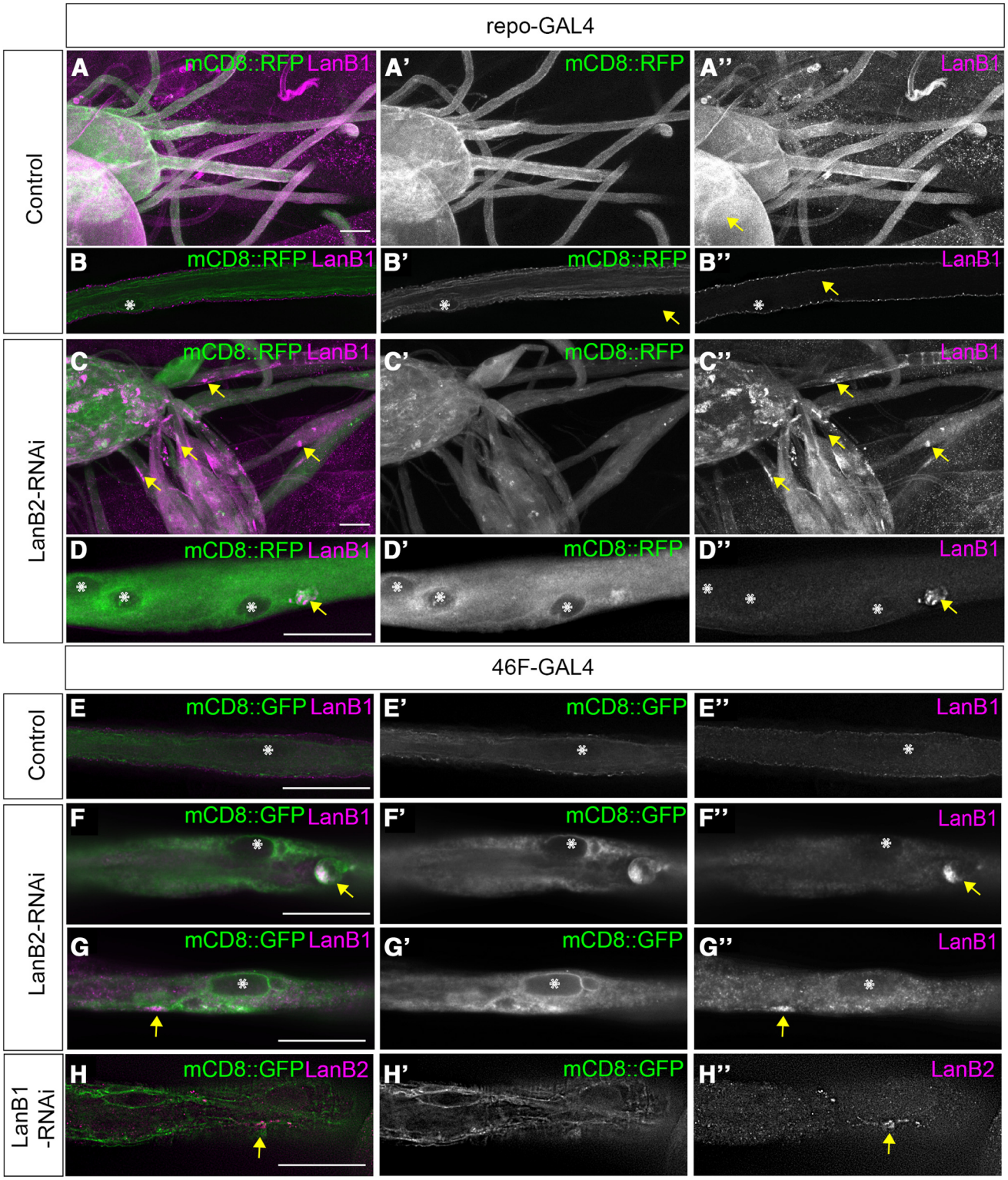

Figure 2. LanB2 knockdown results in LanB1 accumulation in glia. ***A–D***, Peripheral nerves of control (***A***, ***B***) and *repo>LanB2-RNAi* larvae (***C***, ***D***). Glia were labeled with mCD8::RFP (green) and immunolabeled for anti-LanB1 (magenta). ***A***, ***C***, Low-magnification images of peripheral nerves and ventral nerve cord. ***B***, ***D***, Higher-magnification images of individual peripheral nerves in longitudinal sections. Asterisks mark nuclei and arrows mark LanB1 accumulations. Scale bars, 30 μm. ***E–G***, Longitudinal sections of peripheral nerves in control (***E***) and *46F>LanB2-RNAi* larvae (***F***, ***G***). Glia were labeled with mCD8::GFP (green) and immunolabeled with anti-LanB1 antibody (magenta). Asterisks mark nuclei and arrows mark LanB1 accumulations. Scale bars, 30 μm. ***H***, Nerve from *46F>LanB1-RNAi* larvae with glia labeled with mCD8::GFP (green) and immunolabeled with anti-LanB2 antibody (magenta). Arrows mark LanB2 accumulations. Scale bar, 30 μm.

and location of the KDEL::GFP-positive aggregates within perineurial glia matched the areas of expanded ER we observed ultrastructurally. The localization of LanB1 within these aggregates suggested unbound LanB1 accumulated in the ER, leading to ER expansion and possibly to ER stress. To test this, we used an ER stress marker where *Discosoma* red fluorescent protein (dsRed) is placed under the control of the promoter for XBP1 (Ryoo et al., 2013). ER stress, the unfolded protein response, and

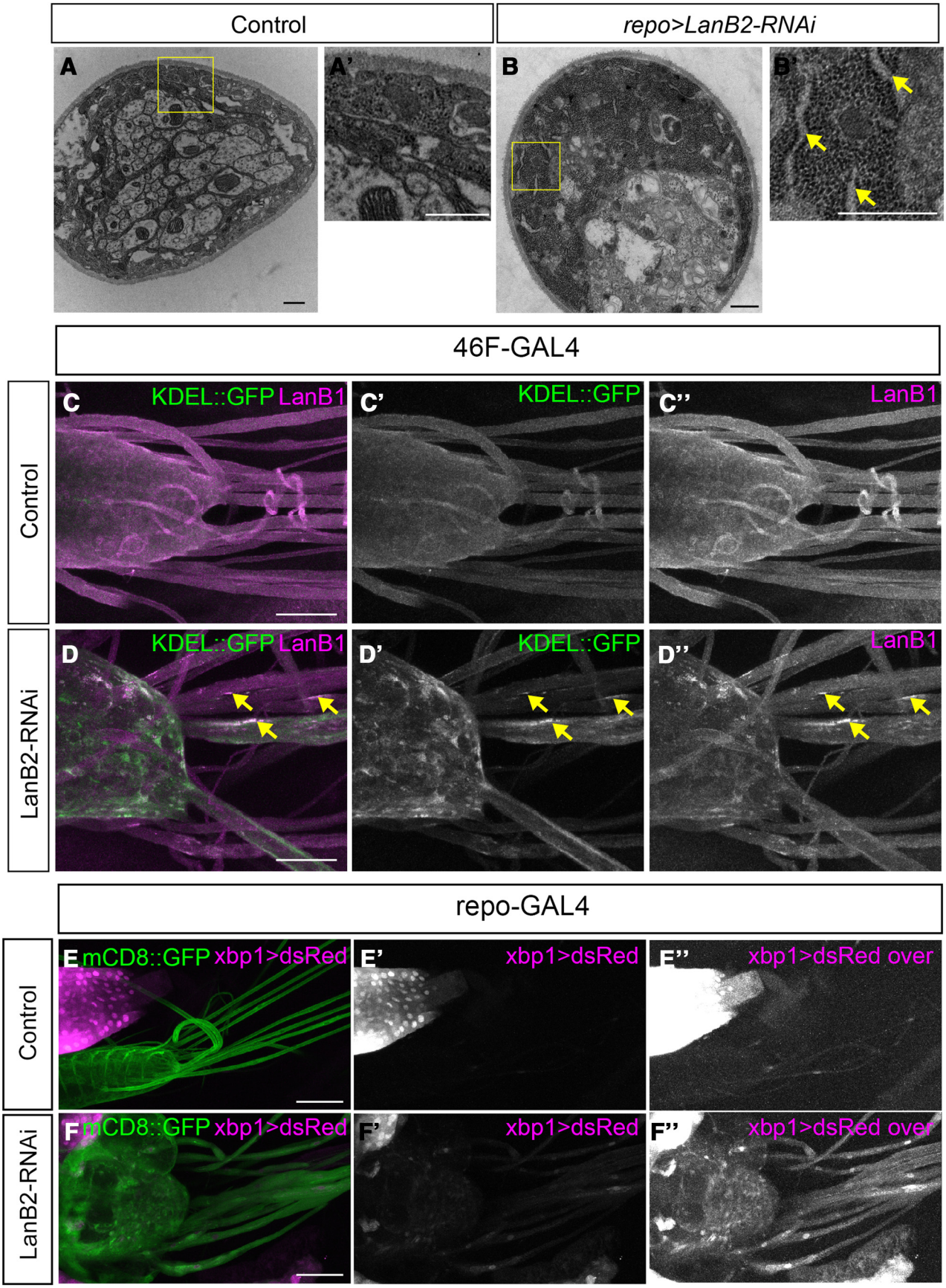

Figure 3. Loss of LanB2 leads to increased ER, LanB1 aggregates, and ER stress. ***A***, ***B***, TEM images of peripheral nerve section. ***A***, Control nerves show the normal distribution of ribosomes in perineurial glia. ***B***, *repo>LanB2-RNAi*-generated swollen perineurial glia with increased density of ribosomes and areas of distended ER. Yellow boxes are shown digitally magnified in ***A'*** and ***B'*** and yellow arrows point to areas of distended ER. Scale bars, 500 nm. ***C***, ***D***, The ventral nerve cord and peripheral nerves of larvae where the perineurial glia (*Figure legend continues.*)

high protein secretory load increases transcription from the XBP1 promoter and causes an increase in the expression of dsRed. When expressed in all glia using *repo-Gal4*, we found that glial cells exhibit almost no XBP1 transcription under control conditions (Fig. 3*E*). However, upon LanB2 knockdown in glia, XBP1 activation via dsRed expression was visible (Fig. 3*F*). Our findings suggest that the loss of LanB2 leads to accumulation of LanB1 within the ER and results in ER stress. We hypothesized that if accumulation of LanB1 results in ER accumulation, then overexpression of LanB1 in perineurial glia using a UAS-LanB1 [an EP insertion in LanB1, *LanB1[EP-600]*, that drives LanB1 expression (de Celis and Molnar, 2010)] would result in ER aggregates. Consistently, we found that the expression pattern of KDEL-GFP in *46F>LanB1* larvae demonstrated that the ER was increased and aggregated compared with control larvae (Fig. 4*F*,*G*), very similar to the phenotype seen after LanB2 knockdown in perineurial glia. Finally, when LanB1 was overexpressed in all glia using *repo-GAL4*, glia in all larvae ($n = 10$) demonstrated vacuoles similar to those observed with LanB2 knockdown (Fig. 4*H*,*I*).

Tango1 mediates laminin secretion via a collagen-independent mechanism

Most proteins are secreted from the ER to Golgi via small COPII (coatomer protein II) vesicles (50–60 nm). However, ECM components, such as collagen and laminin, are too large to be secreted in these vesicles. While the mechanism of laminin secretion remains unknown, collagen secretion has been investigated and a transmembrane ER protein, Tango1, has been found to mediate secretion of many types of collagen (Wilson et al., 2011). By binding to collagen and simultaneously delaying COPII vesicle budding from ER exit sites, Tango1 accommodates the budding of larger COPII vesicles containing collagen from the ER (Saito et al., 2009; Malhotra and Erlmann, 2011). We hypothesized that an analogous mechanism might be used by glia to secrete laminin. Using an RNAi known to specifically target Tango1 (Lerner et al., 2013), we found that expression of Tango1 RNAi in all glia, and perineurial glia specifically, resulted in intracellular LanB2 and LanB1 accumulations (Fig. 4*C*,*D*). The LanB1 accumulations colocalized with GFP-labeled ER aggregates identified with KDEL::GFP (Fig. 4*E*). We screened other members of the Tango family (Tango6, Tango7, Tango5, Tango9, and Tango14; Bard et al., 2006) by expressing RNAi constructs against each in glia (data not shown) and found that only Tango1 RNAi affected laminin secretion. Previous models of Tango1 function suggest that laminin accumulates passively in COPII vesicles by following Tango1-mediated secretion of collagen (Lerner et al., 2013). In *Drosophila*, collagen IV is not observed within the peripheral glia (Xie and Auld, 2011; Fig. 5*A*,*B*), and is deposited by circulating hemocytes and fat bodies (Bunt et al., 2010; Pastor-Pareja and Xu, 2011). We examined the effect of Tango1 knockdown on Viking::GFP, the *Drosophila* homolog of collagen IV endogenously tagged with GFP (Morin et al., 2001). Tango1 RNAi expressed in perineurial glia affected laminin secretion with accumulation of LanB2 within the glial cell (Fig. 5*C*,*D*), but had no impact on the external localization of Viking::GFP in the PNS, nor did we observe any accumulations of Viking::GFP within the cytosol of the peripheral glia (Fig. 5*C*,*D*). Our results confirm that Viking::GFP is not secreted by glia and suggest that Tango1 is capable of mediating laminin secretion independent of collagen. The results also suggest two possibilities: that Tango1 and laminin may bind directly to trigger large vesicle formation, or that Tango1 may have a more ubiquitous role in large vesicle formation than previously thought.

Overall we observed that knockdown of Tango1 had differential effects on peripheral nerves compared with LanB2 RNAi. Tango1 RNAi was lethal only using *repo-GAL4* (not with *46F-GAL4*) and did not result in glial swelling using either GAL4 driver (Table 1; Fig. 6*E*). Knockdown of LanB2 had a more substantial effect on glial structure than knockdown of Tango1, possibly because the Tango1-RNAi transgene may be less effective. Alternatively it is likely that laminin subunits are able to successfully form the laminin heterotrimer in the absence of Tango1, but not LanB2, suggesting that it is the unbound LanB1 in glia expressing LanB2 RNAi that resulted in the more severe consequences.

Reduction of LanB1 rescues swelling due to LanB2 knockdown

Although knockdown of both LanB2 and Tango1 results in accumulation of LanB1 intracellularly, our results and those of previous studies suggest that knockdown of LanB2 resulted in the retention of unbound LanB1 monomers while knockdown of Tango1 resulted in the retention of the entire laminin heterotrimer (Yurchenco et al., 1997; Lerner et al., 2013). We noted that knockdown of LanB2, but not Tango1, caused glial swelling, suggesting that unbound LanB1 within the ER may be more deleterious than accumulation of laminin heterotrimers (Fig. 6*A*,*B*,*D*). To quantify this difference, the diameters of peripheral nerves were measured at the widest point within 300 μm of the ventral nerve cord (Fig. 6*E*). The maximum nerve diameters in control larvae (*repo>mCD8::RFP*) measured on average 10.42 μm ($n = 72$) (Fig. 6*A*). Expression of Tango1 RNAi did not result in significantly swollen nerves, with an average diameter of 11.73 μm ($n = 74$) (Fig. 6*D*). In contrast, expression of LanB2 RNAi resulted in nerves that were significantly wider than controls and had an average maximum width of 20.23 μm ($n = 44$) (Fig. 6*B*). To further determine whether this swelling was due to an intracellular accumulation of unpaired LanB1 monomers, we compared widths of *repo>LanB2-RNAi* nerves in a heterodeficient LanB1 background (*Df(2L)Exel7032L/+*) to widths of *repo>LanB2-RNAi* expression alone. We found that reducing the gene dose of LanB1 by half resulted in significantly less swollen nerves (Fig. 6*C*) with an average width of 16.13 μm ($n = 45$). Together with the lack of swelling due to Tango1 RNAi, our findings suggest that external depletion of glial-derived laminin heterotrimers and subsequent reduced laminin signaling does not initiate glial swelling. Rather, the reduced swelling seen after the simultaneous reduction of LanB1 and LanB2 suggests that the swelling is due to the accumulation of unbound intracellular LanB1.

LanB2, but not Tango1, knockdown in glia disrupted larval movement

The lethality associated with LanB2 knockdown implies that the unbound LanB1 monomers accumulating in glia are not

←

(*Figure legend continued.*) ER was labeled using *46F>KDEL::GFP* (green) and immunolabeled with anti-LanB1 antibody (magenta). ***C***, Distribution of KDEL::GFP and LanB1 is uniform and diffuse in control nerves. ***D***, Colocalization of LanB1 accumulations and ER aggregates was observed in *46F>LanB2-RNAi* (yellow arrows). Scale bars, 50 μm. ***E***, ***F***, Ventral nerve cord and peripheral nerves were labeled using *repo>mCD8::GFP* and xbp1 expression was visualized using the *xbp1>dsRed* expression reporter. Control, *repo-GAL4* (***E***) had weak levels of dsRed in the glia while *repo>LanB2-RNAi* (***F***) showed increased dsRed expression. The red channel was overexposed equally in ***E″*** and ***F″*** to show differences in xbp1 expression. Scale bars, 100 μm.

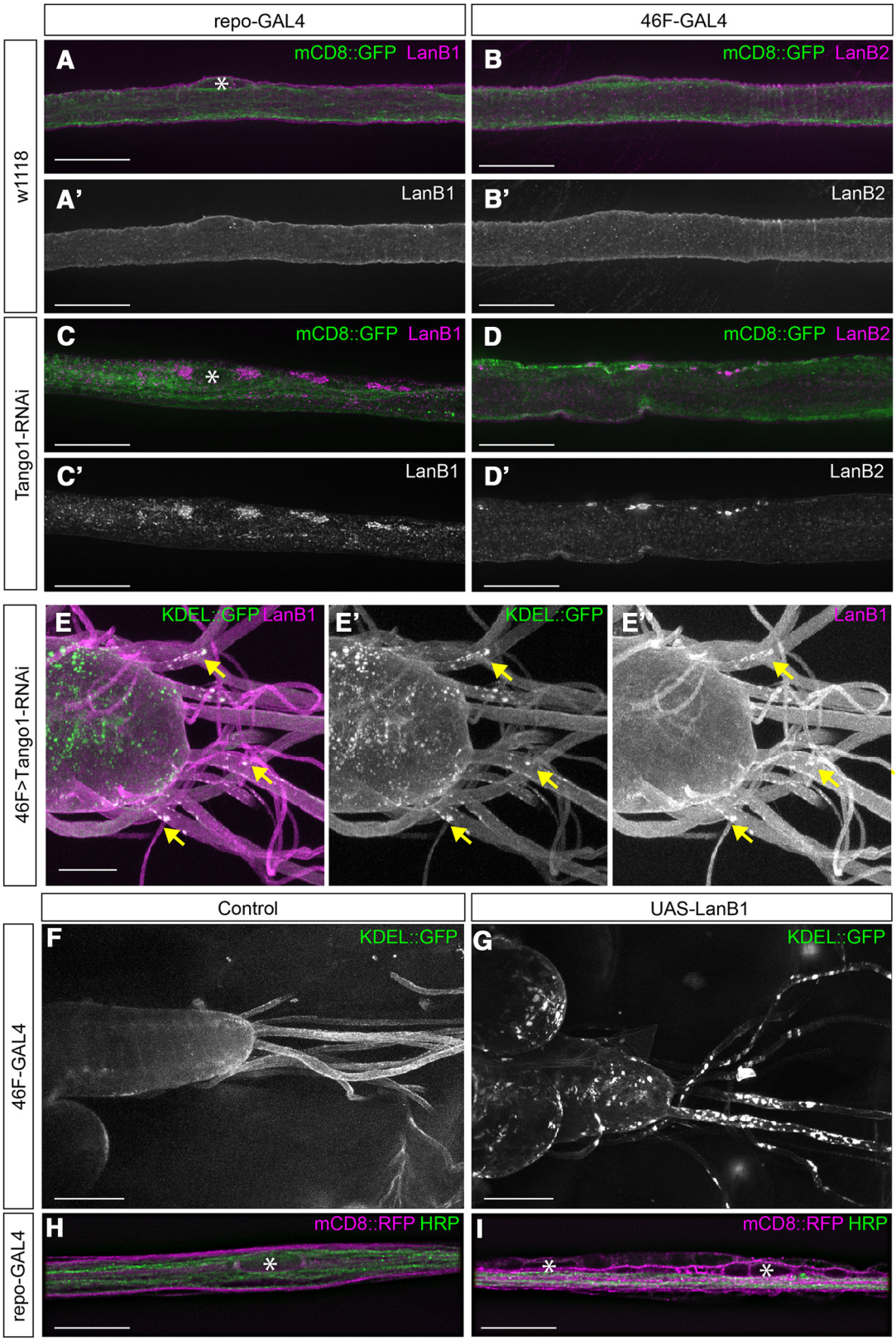

Figure 4. Knockdown of Tango1 leads to accumulations of LanB1 and LanB2. ***A***, ***B***, High-magnification images of control *repo-GAL4* (***A***) and *46F-GAL4* (***B***) peripheral nerves with glial membranes labeled with mCD8::GFP (green) and immunolabeled with LanB1 (***A***, magenta) or LanB2 (***B***, magenta). ***C***, ***D***, *repo>Tango1-RNAi* (***C***) and *46F>Tango1-RNAi* (***D***) peripheral nerves demonstrate accumulations of LanB1 and LanB2 when Tango1 is knocked down (arrows). Nuclei are marked by asterisks. Scale bars, 20 μm. ***E***, The ventral nerve cord and peripheral nerves of larvae where the perineurial glia driver *46F-GAL4* drove the expression of ER marker KDEL::GFP (green) and Tango1 RNAi. Colocalization of LanB1 accumulations (magenta) and ER aggregates was observed (yellow arrows). Scale bars, 50 μm. ***F***, ***G***, Low-magnification images of CNS and nerves with *46F-GAL4* driving KDEL::GFP without (***F***) or with (***G***) overexpression of LanB1 using *UAS-LanB1*$^{EP\text{-}600}$, resulting in ER aggregates. Scale bars, 100 μm. ***H***, High-magnification images of control nerves with glial membrane labeled with mCD8::RFP (magenta) and axons immunolabeled using anti-HRP antibody (green). ***I***, Nerves with overexpression of LanB1 in glia, *repo>LanB1*$^{EP\text{-}600}$, demonstrated vacuoles. Nuclei are marked by asterisks. Scale bars, 15 μm.

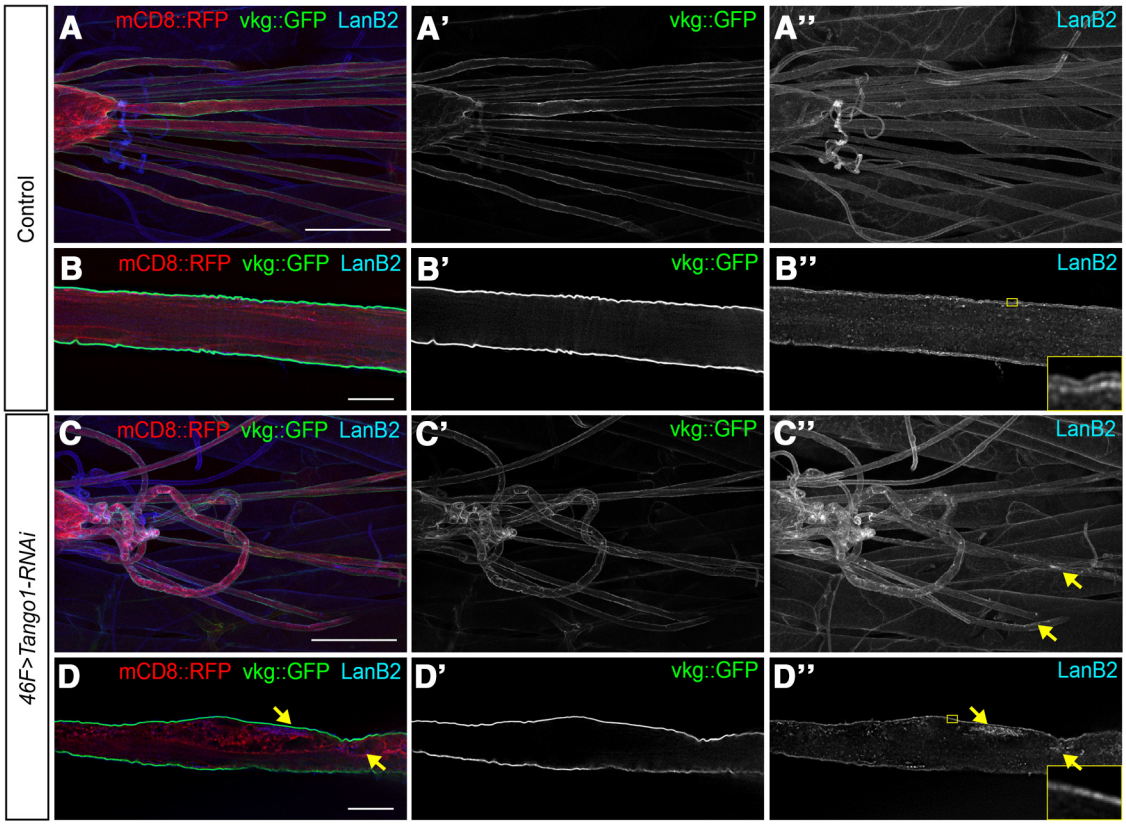

Figure 5. Tango1 mediates laminin secretion via a collagen-independent mechanism. ***A***, Low-magnification image of control ventral nerve cord and peripheral nerves in larvae with *46F-GAL4* driving mCD8::RFP in perineurial glia (red), and collagen-IV endogenously tagged with GFP and Viking::GFP (green), and immunolabeled for LanB2 (blue). Scale bar, 100 μm. ***B***, High-magnification image of nerve section in ***A***. Scale bar, 15 μm. Digitally magnified section of ECM in inset shows two distinct layers of LanB2. Viking::GFP is not observed in the interior of the nerve. ***C***, Low-magnification image of ventral nerve cord and peripheral nerves in *46F>Tango1-RNAi* larvae with the perineurial glia membrane labeled with mCD8::RFP (red) and Viking::GFP (green), and immunolabeled for LanB2 (blue). Loss of Tango1 led to accumulations of LanB2 (yellow arrows) but not Viking::GFP. Scale bar, 100 μm. ***D***, High-magnification image of a nerve in ***C***. Scale bar, 15 μm. Digitally magnified section of ECM in inset shows one layer of LanB2. Viking::GFP was not observed in the interior of the nerve, while LanB2 was observed in intracellular accumulations (yellow arrows).

only affecting glial morphology, but also glial function. To determine whether the morphological defects caused by LanB2 knockdown in glia were associated with significant physiological defects, we assayed larval locomotion. The speeds of third-instar larvae over a period of 15 s were recorded using an adapted "multiworm tracker" system (Swierczek et al., 2011). This system records and quantifies the movements of multiple larvae simultaneously over a defined period of time. Control larvae (*repo-GAL4*) moved at an average speed of 3.69 mm/s (Fig. 6*F*). Using this system, we found that *repo>LanB2-RNAi* larvae were almost immobile with an average speed of 0.32 mm/s. Before tracking, all larvae were confirmed to be alive, to exhibit feeding behavior, and to respond to touch by rolling or bending. However, *repo>Tango1-RNAi* larvae were not significantly slower than controls and had an average speed of 3.16 mm/s (Fig. 6*F*). We also recorded the instantaneous speed of *repo>LanB2-RNAi* larvae in a *LanB1*-heterodeficient background. While these larvae had an improved average speed of 0.74 mm/s, this was not significantly different from *repo>LanB2-RNAi* larvae (Fig. 6*F*) and both genotypes were lethal in late third-instar stages (Table 1). Although reducing the gene dose of LanB1 by half significantly diminished the degree of glial swelling, it was not sufficient to significantly rescue larval locomotion, and glial function is likely still disrupted even with a reduction in LanB1.

Effects of LanB2 knockdown on perineurial and wrapping glia

As with *repo-GAL4*-driven knockdown of LanB2, knockdown of LanB2 in the perineurial glia using *46F-GAL4* also resulted in lethality. While the function of the perineurial glia is not known, expression of two initiators of apoptosis, *hid* and *rpr*, under UAS/GAL4 control with *46F-GAL4* resulted in early larval lethality (Table 1). We used a temperature-sensitive GAL80 to control expression and, when shifted to 29°C for 24 h, *46F>hid,rpr* larvae survived to third instar but were completely immobile. This finding suggests that perineurial glia are critical for nervous system function. The effects of LanB2 knockdown in this subtype of glia was tested using the multiworm tracker system. The average speed of *46F>LanB2-RNAi* larvae was 2.60 mm/s, which is significantly lower than the average speed of controls (*46F-GAL4*), 3.73 mm/s (Fig. 7*A*). Although significantly slower than controls, *46F>LanB2-RNAi* larvae were still mobile, unlike *repo>LanB2-RNAi* larvae. This is likely due to LanB2-RNAi expression in all glia and the earlier expression of *repo-GAL4* (which begins in embryogenesis), whereas *46F-GAL4* is expressed later in perineurial glia [which arise in the last embryonic stages (von Hilchen et al., 2013)]. It may be that laminin is expressed by other glia and loss of LanB2 in these other layers contributes to the immobility seen in *repo>LanB2-RNAi* larvae. Wrapping glia directly contact and ensheath axons, making it an ideal candidate for affecting signal transmission and larval movement. Ultra-

structural analysis of *repo>LanB2-RNAi* nerves using TEM revealed that the wrapping glia had severe morphological defects, including vacuole-like structures and a lack of processes extending around axons (Fig. 7*C*,*F*). To determine whether this was cell-autonomous or an indirect effect on wrapping glia, we expressed LanB2 RNAi using the wrapping glia driver, *nrv2-GAL4*, and analyzed wrapping glial morphology by coexpression of cytosolic GFP. We observed vacuole-like structures near the wrapping glia nuclei and a lack of processes extending between nuclei (Fig. 7, compare *D*,*E*, *G*,*H*). However, accumulations of LanB1 within wrapping glia could not be detected (data not shown). Normally wrapping glia extend processes to wrap around and along each axon with processes from neighboring wrapping glia overlapping to form a continuous glial cover along the length of the nerve (Fig. 7*C*,*E*,*K*). This extensive network of wrapping glial processes was reduced when LanB2 was knocked down in the wrapping glia. For quantification, disruption was defined by measuring the processes from different wrapping glia that did not overlap, resulting in gaps in the glial coverage or discontinuous processes along the length of the axon (Fig. 7*F*,*H*,*J*). The morphological defects observed with LanB2 RNAi were quantified by comparing the percentage of nerves in which vacuole-like structures were observed and the percentage of nerves in which wrapping glial processes were discontinuous (Fig. 7*I*). We observed a significant increase in both vacuole-like structures and breaks or discontinuous wrapping glial processes compared with controls (*nrv2-GAL4*). These results clearly demonstrate that LanB2 knockdown specifically in wrapping glia has a cell-autonomous effect on glial morphology. To determine whether the morphological defects were physiologically significant, the average speeds of control (*nrv2-GAL4*) and *nrv2>LanB2-RNAi* larvae were measured using the multiworm tracker system. Surprisingly, we found that there was no significant difference in speed between control and *nrv2>LanB2-RNAi* larvae (Fig. 7*B*). However, we cannot exclude a more subtle effect on locomotion. Furthermore, we observed that knockdown of LanB2 RNAi in wrapping glia resulted in viable adults (Table 1). To verify that wrapping glia were indeed important for locomotion and larval survival, we expressed the initiators of apoptosis, *hid* and *rpr*, using *nrv2-GAL4* and found that the larvae were significantly slower (Fig. 7*B*) and died during pupal stages (Table 1). These results suggest that either the loss of *nrv2-GAL4*-expressing cells at sites other than the PNS is fatal or that the wrapping glia maintain an essential function even with the LanB2 RNAi induced morphological defects. Overall, these results suggest that loss of LanB2 leads to a disruption in wrapping glia morphology, including loss of the glial wrap and the appearance of gaps between neighboring wrapping glial cells, but that these defects do not disrupt peripheral nerve function.

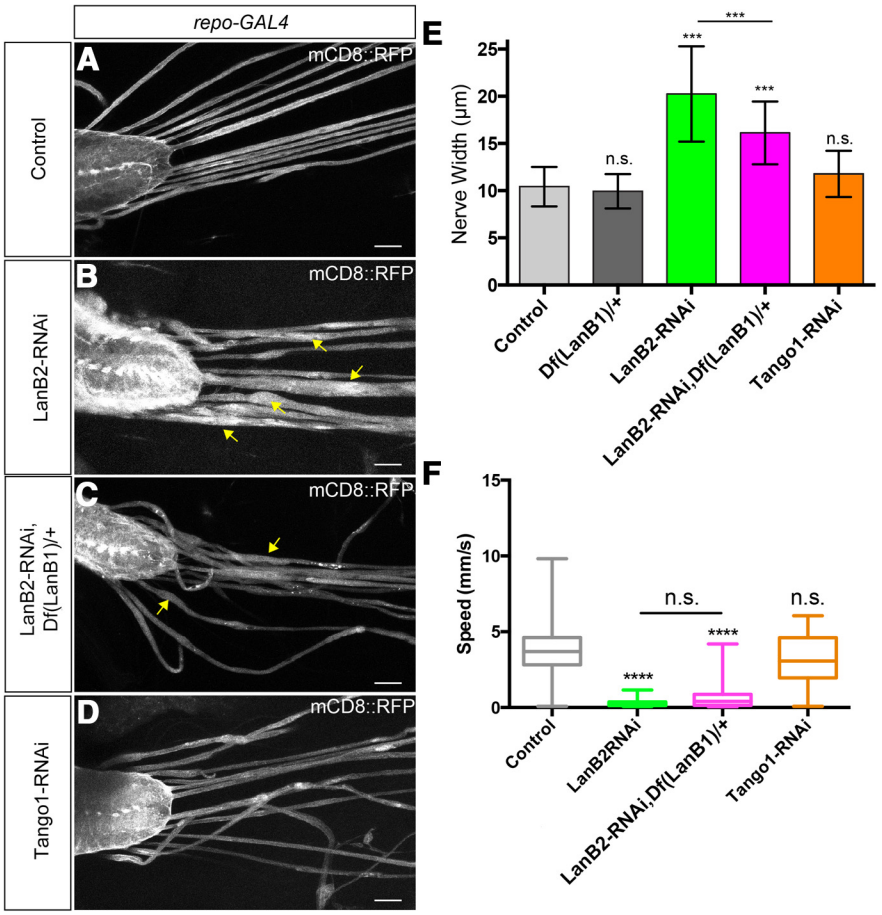

Figure 6. LanB2 but not Tango1 knockdown generates glial swelling and locomotion defects. ***A–D***, The ventral nerve cord and peripheral nerves with glial membranes labeled with mCD8::RFP. ***A***, Control *repo-GAL4*; ***B***, *repo>LanB2-RNAi*; ***C***, *repo>LanB2-RNAi* heterozygous for a LanB1 deficiency; ***D***, *repo>Tango1-RNAi*. Arrows indicate areas of swelling. Scale bars, 50 μm. ***E***, The mean width of the widest section of peripheral nerves in control, *repo-GAL4*, versus *repo>RNAi* lines shown in ***A–D***. Mean widths were as follows: controls, 10.42 $\pm$ 2.09 μm, $n = 72$; *Df(LanB1)/+* heterozygotes, 9.94 $\pm$ 1.82 μm, $n = 42$, $p = 0.923$; *repo>LanB2-RNAi*, 20.23 $\pm$ 5.04 μm, $n = 44$, $p < 0.0001$; *repo>LanB2-RNAi, Df(LanB1)/+*, 16.13 $\pm$ 3.33 μm, $n = 45$, $p < 0.0001$; *repo>Tango1-RNAi*, 11.73 $\pm$ 2.45 μm, $n = 74$, $p = 0.054$. Differences in mean width was analyzed using a one-way ANOVA and Tukey's *post hoc* test and significance compared with control shown for each experiment (N.S., not significant; ***$p < 0.001$). Mean widths between *repo>LanB2-RNAi* and *repo>LanB2-RNAi, Df(LanB1)/+* were significantly different ($p < 0.001$). ***F***, Average instantaneous larval speed of control (*repo-GAL4*) versus *repo>*RNAi lines. For each box-and-whisker plot, the box represents the first and third percentiles, the middle line the median, and the whiskers are the minimum and maximum. Larval speeds: control, 3.69 $\pm$ 1.73 mm/s, $n = 118$; *repo>LanB2-RNAi*, 0.32 $\pm$ 0.26 mm/s, $n = 35$; *repo>LanB2-RNAi,Df(LanB1)/+*, 0.74 $\pm$ 0.96 mm/s, $n = 56$; *repo>Tango1-RNAi*, 3.16 $\pm$ 1.55 mm/s, $n = 34$. Knockdown of LanB2 alone ($p < 0.0001$) and in *Df(LanB1)/+* heterozygotes ($p < 0.0001$) resulted in larvae that were significantly slower than controls while knockdown of Tango1 ($p = 0.2117$) did not significantly affect larval speed. The difference between *repo>LanB2-RNAi* alone and in a *Df(LanB1)/+* heterozygous background was not significant ($p = 0.518$).

Discussion

The role of laminin and the ECM in glial wrapping has been investigated in vertebrate systems by examining the gross morphological and molecular changes induced by knocking out individual laminin subunits in glia. A decrease in glial wrapping, proliferation, and survival was attributed to a lack of laminin binding to various receptors, including integrins, dystroglycan, and syndecans. However, it was found that knock-out of laminin resulted in more severe phenotypes than the additive phenotypes of multiple-receptor knock-out studies (Yu et al., 2005). In this paper, we present evidence that eliminating one laminin subunit

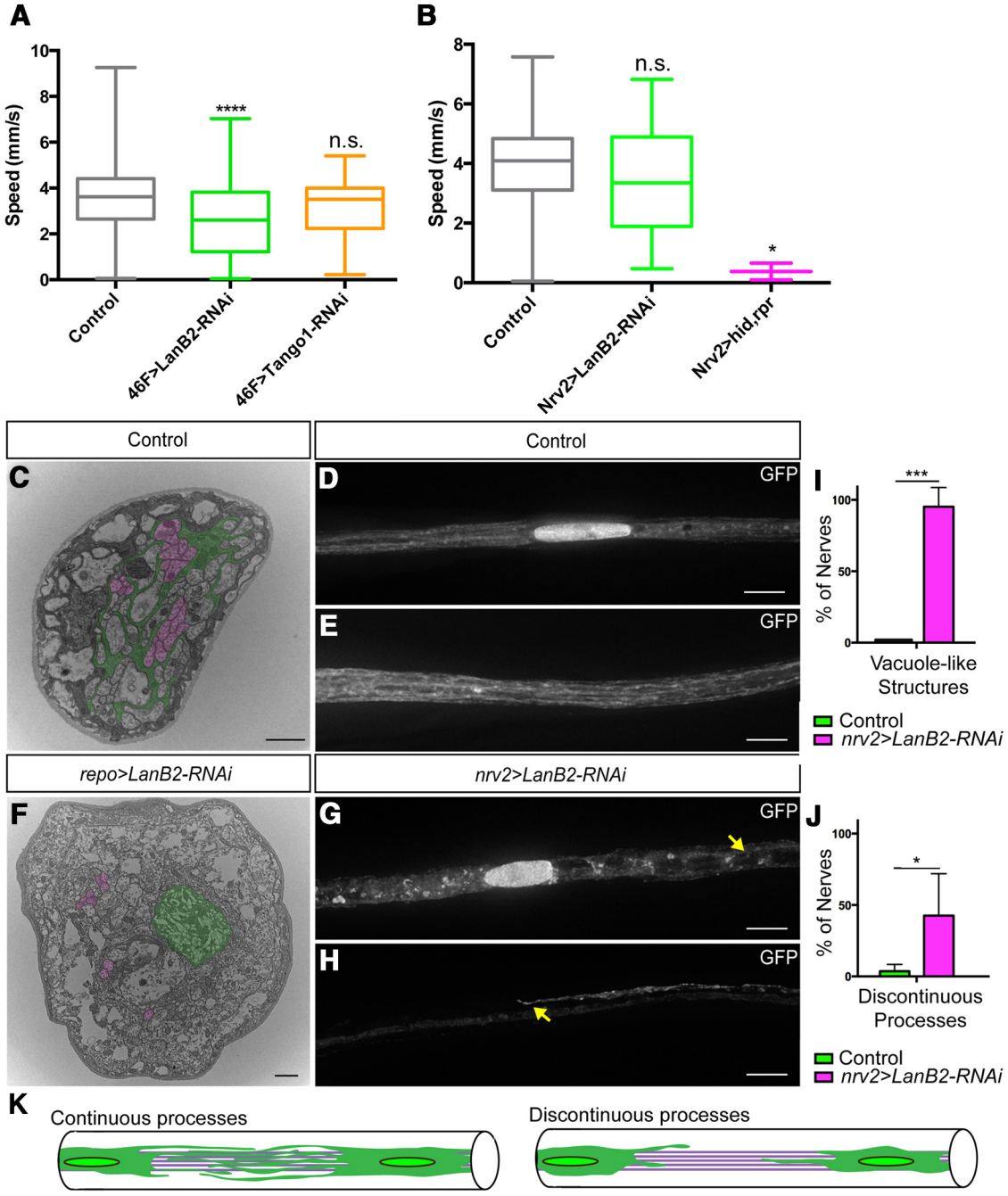

Figure 7. Effects of LanB2 knockdown on perineurial and wrapping glia. ***A***, Average instantaneous larval speed of control (*46F-GAL4,* gray) and *46F*>RNAi lines. Larval speeds were as follows: control, 3.73 ± 1.79 mm/s, $n = 116$; *46F*>*LanB2-RNAi*, 2.60 ± 1.65 mm/s, $n = 58$); *46F*>*Tango1-RNAi*, 3.13 ± 1.40 mm/s, $n = 22$. Knockdown of Tango1 ($p = 0.281$) did not significantly affect speed. Knockdown of LanB2 resulted in significantly slower larvae ($p = 0.0002$). For each box-and-whisker plot, the box represents the first and third percentiles, the middle line the median, and the whiskers are the minimum and maximum. ***B***, Average instantaneous larval speed of control (*nrv2-GAL4*), *nrv2*>*LanB2-RNAi*, and *nrv2*>*hid,rpr* lines. There was no significant difference between controls (3.87 ± 1.64 mm/s, $n = 74$) and *nrv2*>*LanB2-RNAi* (3.42 ± 1.78 mm/s, $n = 50$, $p = 0.310$). There was a significant difference between controls and *nrv2*>*hid,rpr* (0.38 ± 0.40 mm/s, $n = 2$, $p = 0.013$). ***C***, ***F***, TEM of peripheral nerve sections from control *repo-GAL4* and *repo*>*LanB2-RNAi* nerves. Wrapping glia were false-colored green and a selection of axons were false-colored magenta. Control wrapping glia extended processes around axons (***C***), while wrapping glia in *repo*>*LanB2-RNAi* nerves did not (***F***). Scale bars, 1 μm. ***D***, ***E***, Projection images of control peripheral nerves with *nrv2-GAL4* driving GFP expression in wrapping glia near nuclei (***D***) and between nuclei (***E***) demonstrate the extensive wrapping glial processes within the core of the nerve. Scale bars, 15 μm. ***G***, ***H***, Projection images of peripheral nerves in *nrv2*>*LanB2-RNAi* larvae near a nucleus (***G***) and between nuclei (***H***) demonstrate vacuole-like structures (***G***, arrow) and discontinuous processes (***H***, arrow) that illustrate the failure of neighboring wrapping glia to connect and ensheath the peripheral axons. Scale bars, 15 μm. ***I***, Quantification of the wrapping glial morphological defects in control *nrv2-GAL4* versus *nrv2*>*LanB2-RNAi* nerves. Control nerves ($n = 55$) had significantly less vacuole-like structures compared with *nrv2*>*LanB2-RNAi* nerves ($n = 47$, $p < 0.001$). ***J***, Control nerves had no evidence of discontinuous processes ($n = 47$), while a significantly higher percentage of *nrv2*>*LanB2-RNAi* nerves did ($n = 21$, $p < 0.001$). Error bars are SD. ***K***, Diagram depicting continuous processes in control nerves seen by overlapping glial processes (green) between two wrapping glial nuclei (green circle) covering axons (gray). Discontinuous processes are defined as glial processes that do not overlap between two wrapping glial nuclei.

causes cellular changes that go beyond the loss of receptor-ligand signaling and contribute to glial mutant phenotypes.

We have demonstrated that glial cells expressing RNAi against three different laminin subunits result in morphological defects. Knockdown of the laminin γ subunit LanB2 results in extensively swollen glia, accumulation of LanB1 in the ER, and expanded ER, leading to ER stress with disrupted intracellular morphology, including vacuole-like structures. In laminin assembly, the β-γ dimer is formed followed by α chain recruitment where trimer formation is necessary for transport through the Golgi and secretion (Morita et al., 1985; Peters et al., 1985; Aratani and Kitagawa, 1988). Studies *in vitro* and in *C. elegans* found intracellular accumulation of the γ laminin subunit in the absence of the β subunit (Yurchenco et al., 1997; Huang et al., 2003; Kao et al., 2006). However, the subcellular localization and physiological consequences of the intracellular laminin accumulations was not determined. Our analysis of the knockdown of the γ subunit (LanB2) in all glia extended this line of study and found that loss of LanB2 led to β subunit (LanB1) accumulations, ER expansion, and ER stress. Glial swelling due to LanB2 knockdown was correlated with excess LanB1, and the swollen glial phenotype was partially rescued by introducing a heterozygous LanB1 deficiency in the background, effectively halving the amount of LanB1 available for translation. The partial rescue in glial swelling due to LanB1 heterodeficiency supports the hypothesis that unbound LanB1 is acting as a misfolded protein in the ER to induce the unfolded protein response and ER stress. In further support, we found overexpression of LanB1 alone resulted in ER aggregates and vacuoles in glia. Knockdown of Tango1, a protein known to mediate ER exit of collagen (Malhotra and Erlmann, 2011), resulted in LanB1 and LanB2 accumulations in the ER. Tango1 knockdown results in laminin retention in *Drosophila* ovary follicle cells. However, the subcellular localization of laminin was not demonstrated (Lerner et al., 2013). Our results refine these observations as both LanB2 and Tango1 knockdown result in LanB1 accumulations specifically in the expanded ER. However, while LanB2-RNAi led to severe glial swelling and locomotion defects, expression of Tango1 RNAi did not. In the case of Tango1 RNAi, this is possibly due to Tango1 knockdown inhibiting secretion of assembled laminin heterotrimers. Previously, Tango1 has been implicated primarily in collagen secretion (Malhotra and Erlmann, 2011) and we found Tango1 mediates laminin secretion in the absence of collagen IV in perineurial glia. Our findings imply that there may be a Tango1-specific binding site on laminin or that Tango1 may play a broader role in protein secretion than previously thought. Together, our findings suggest that the glial defects observed after LanB2 knockdown are due to excess amounts of unbound LanB1 monomers in the ER causing ER stress. Alternatively, the increased LanB1 and ribosomal content in these areas may indicate increased translation due to glia sensing inadequate amounts of external laminin.

The glial defects we observed are likely due to disruption of laminin secretion, but it is possible that the defects we observed were in part due to loss of laminin from the extracellular space and loss of ECM receptor signaling, such as integrin signaling. We favor the first explanation as blocking the secretion of the laminin trimer by Tango1 RNAi did not result in glial swelling, suggesting that the reduction in laminin secretion did not lead to glia disruption. Loss of integrins and metalloproteinase-mediated degradation of the surrounding ECM does not lead to glial swelling or formation of vacuoles, but rather triggers a loss of perineurial glia wrapping of the axon (Xie and Auld, 2011). In *Drosophila*, the fat body and hemocytes contribute to the deposition of ECM proteins in the basement membrane surrounding the nervous system (Bunt et al., 2010; Pastor-Pareja and Xu, 2011), explaining why the loss of laminin secretion from glia in Tango1 does not lead to the same phenotypes as integrin knockdown.

This raises the interesting question of why *Drosophila* glia secrete laminin and not other ECM proteins. Similarly, why do *Drosophila* wrapping glia, which do not contact a basement membrane, express laminin? Wrapping glia were morphologically affected by LanB2 knockdown. However. accumulations of LanB1 within wrapping glia were not seen, implying that wrapping glia express low levels of laminin. With the available antibodies, it is difficult to detect and assess the levels of laminin between axons and wrapping glia or between wrapping and subperineurial glia. The presence of laminin interior to the nerve is supported by previous experiments where integrin knockdown in wrapping glia resulted in a lack of process extension (Xie and Auld, 2011) similar to that seen after LanB2 knockdown, suggesting that integrin may bind to laminin present between axons and wrapping glia or between wrapping and subperineurial glia. Although LanB2 knockdown in wrapping glia resulted in morphological defects, including decreased wrapping, third-instar larvae exhibited no mobility defects and even survived to adulthood and this is also true of integrin knockdown in the wrapping glia (data not shown). The surprising finding that full contact between wrapping glia and peripheral axons is unnecessary for locomotion is consistent with mutants in the Na-K-Cl cotransporter, Ncc69. *Ncc69* mutant larvae have significant osmotic swelling that inhibits direct contact between axons and the wrapping glia and yet these larvae had normal action potential activity and survived to adult stages (Leiserson et al., 2011). Apoptosis-induced death of the wrapping glia did, however, result in a total lack of mobility and lethality, indicating that either the wrapping glia or other *nrv2-GAL4*-expressing cells are essential to survival and locomotion.

Larval survival and mobility were affected by knockdown of LanB2 in perineurial glia, a glial subtype that does not directly contact axons. Perineurial glia are born late in embryogenesis, surround the CNS and PNS during larval stages (von Hilchen et al., 2013), and have been implicated in ECM remodeling during nervous system growth (Stork et al., 2008; Meyer et al., 2014). Here, we demonstrate that perineurial glia secrete laminin, but not collagen IV, and contribute to nervous system function. The decreased mobility seen in *46F>LanB2-RNAi* larvae provides support for the role of the outer layer of perineurial glia and the ECM in structurally supporting the larval nervous system as these glia do not contact either neuronal cell bodies or axons.

Ultimately, our findings suggest that loss of receptor-ligand signaling is not the sole cause of glial morphological and physiological defects due to loss of laminins. Due to the conserved structure and function of glia across the animal kingdom, it is likely that Schwann cells lacking one subunit of laminin or with a mutation in one subunit affecting laminin trimerization could also demonstrate morphological and functional defects due to the accumulation of unbound laminin subunits leading to ER stress. This could have significant implications as ER stress is important in the pathogenesis of various diseases affecting myelination in the CNS and PNS (Lin and Popko, 2009). This hypothesis has not yet been investigated in vertebrate glia, but it may provide insight into the reasons decreased glial wrapping, proliferation, and survival are seen in vertebrates after knock-out or with inherited mutations in laminin subunits. Schwann cell-specific deletion of *Lamc1* (the γ-1 subunit) leads to a loss of α and β subunit expression and disruption of basement membrane secretion (Yang et

al., 2005; Yu et al., 2005). Loss of γ-1 leads to defects in radial sorting and myelination by myelinating Schwann cells, as well as to loss of proliferation and blocked differentiation in the premyelination stage (Chen and Strickland, 2003; Wallquist et al., 2005; Yang et al., 2005; Yu et al., 2005). Similarly loss of γ-1 leads to the absence of nonmyelinating Schwann cells and the loss of Remak bundles (Yu et al., 2009b). The wrapping glia of *Drosophila* are most similar to nonmyelinating Schwann cells and in these cells loss of the γ subunit led to wrapping defects and ER stress. Whether the loss of the vertebrate γ-1 subunit leads to ER stress that results in the loss of nonmyelinating Schwann cells has not been determined. However, our findings may represent a broader trend in the cellular response to unequal expression of related subunits that together comprise a multimeric protein, such as laminin. Future studies should focus on the effects of ER stress due to mutations in individual subunits of laminin in Schwann cells and other tissues.

References

Aratani Y, Kitagawa Y (1988) Enhanced synthesis and secretion of type IV collagen and entactin during adipose conversion of 3T3–L1 cells and production of unorthodox laminin complex. J Biol Chem 263:16163–16169. Medline

Bard F, Casano L, Mallabiabarrena A, Wallace E, Saito K, Kitayama H, Guizzunti G, Hu Y, Wendler F, Dasgupta R, Perrimon N, Malhotra V (2006) Functional genomics reveals genes involved in protein secretion and Golgi organization. Nature 439:604–607. CrossRef Medline

Bunt S, Hooley C, Hu N, Scahill C, Weavers H, Skaer H (2010) Hemocyte-secreted type IV collagen enhances BMP signaling to guide renal tubule morphogenesis in Drosophila. Dev Cell 19:296–306. CrossRef Medline

Chen YM, Kikkawa Y, Miner JH (2011) A missense LAMB2 mutation causes congenital nephrotic syndrome by impairing laminin secretion. J Am Soc Nephrol 22:849–858. CrossRef Medline

Chen YM, Zhou Y, Go G, Marmerstein JT, Kikkawa Y, Miner JH (2013) Laminin β2 gene missense mutation produces endoplasmic reticulum stress in podocytes. J Am Soc Nephrol 24:1223–1233. CrossRef Medline

Chen ZL, Strickland S (2003) Laminin gamma1 is critical for Schwann cell differentiation, axon myelination, and regeneration in the peripheral nerve. J Cell Biol 163:889–899. CrossRef Medline

de Celis JF, Molnar C (2010) A cautionary tale on genetic screens based on a gain-of-expression approach: the case of LanB1. Fly (Austin) 4:24–29. CrossRef Medline

Dietzl G, Chen D, Schnorrer F, Su KC, Barinova Y, Fellner M, Gasser B, Kinsey K, Oppel S, Scheiblauer S, Couto A, Marra V, Keleman K, Dickson BJ (2007) A genome-wide transgenic RNAi library for conditional gene inactivation in Drosophila. Nature 448:151–156. CrossRef Medline

Durbeej M (2010) Laminins. Cell Tissue Res 339:259–268. CrossRef Medline

Feltri ML, Wrabetz L (2005) Laminins and their receptors in Schwann cells and hereditary neuropathies. J Peripher Nerv Syst 10:128–143. CrossRef Medline

Feltri ML, Graus Porta D, Previtali SC, Nodari A, Migliavacca B, Cassetti A, Littlewood-Evans A, Reichardt LF, Messing A, Quattrini A, Mueller U, Wrabetz L (2002) Conditional disruption of beta 1 integrin in Schwann cells impedes interactions with axons. J Cell Biol 156:199–209. CrossRef Medline

Huang CC, Hall DH, Hedgecock EM, Kao G, Karantza V, Vogel BE, Hutter H, Chisholm AD, Yurchenco PD, Wadsworth WG (2003) Laminin alpha subunits and their role in C. elegans development. Development 130:3343–3358. CrossRef Medline

Kao G, Huang CC, Hedgecock EM, Hall DH, Wadsworth WG (2006) The role of the laminin beta subunit in laminin heterotrimer assembly and basement membrane function and development in C. elegans. Dev Biol 290:211–219. CrossRef Medline

Lee T, Luo L (1999) Mosaic analysis with a repressible cell marker for studies of gene function in neuronal morphogenesis. Neuron 22:451–461. CrossRef Medline

Leiserson WM, Forbush B, Keshishian H (2011) Drosophila glia use a conserved cotransporter mechanism to regulate extracellular volume. Glia 59:320–332. CrossRef Medline

Lerner DW, McCoy D, Isabella AJ, Mahowald AP, Gerlach GF, Chaudhry TA, Horne-Badovinac S (2013) A rab10-dependent mechanism for polarized basement membrane secretion during organ morphogenesis. Dev Cell 24:159–168. CrossRef Medline

Lin W, Popko B (2009) Endoplasmic reticulum stress in disorders of myelinating cells. Nat Neurosci 12:379–385. CrossRef Medline

Malhotra V, Erlmann P (2011) Protein export at the ER: loading big collagens into COPII carriers. EMBO J 30:3475–3480. CrossRef Medline

Meyer S, Schmidt I, Klämbt C (2014) Glia ECM interactions are required to shape the Drosophila nervous system. Mech Dev 133:105–116. CrossRef Medline

Molnar C, López-Varea A, Hernández R, de Celis JF (2006) A gain-of-function screen identifying genes required for vein formation in the Drosophila melanogaster wing. Genetics 174:1635–1659. CrossRef Medline

Morin X, Daneman R, Zavortink M, Chia W (2001) A protein trap strategy to detect GFP-tagged proteins expressed from their endogenous loci in Drosophila. Proc Natl Acad Sci U S A 98:15050–15055. CrossRef Medline

Morita A, Sugimoto E, Kitagawa Y (1985) Post-translational assembly and glycosylation of laminin subunits in parietal endoderm-like F9 cells. Biochem J 229:259–264. CrossRef Medline

Pastor-Pareja JC, Xu T (2011) Shaping cells and organs in Drosophila by opposing roles of fat body-secreted collagen IV and perlecan. Dev Cell 21:245–256. CrossRef Medline

Peters BP, Hartle RJ, Krzesicki RF, Kroll TG, Perini F, Balun JE, Goldstein IJ, Ruddon RW (1985) The biosynthesis, processing, and secretion of laminin by human choriocarcinoma cells. J Biol Chem 260:14732–14742. Medline

Ryoo HD, Li J, Kang MJ (2013) Drosophila XBP1 expression reporter marks cells under endoplasmic reticulum stress and with high protein secretory load. PLoS One 8:e75774. CrossRef Medline

Saito K, Chen M, Bard F, Chen S, Zhou H, Woodley D, Polischuk R, Schekman R, Malhotra V (2009) TANGO1 facilitates cargo loading at endoplasmic reticulum exit sites. Cell 136:891–902. CrossRef Medline

Sepp KJ, Schulte J, Auld VJ (2000) Developmental dynamics of peripheral glia in Drosophila melanogaster. Glia 30:122–133. CrossRef Medline

Sepp KJ, Schulte J, Auld VJ (2001) Peripheral glia direct axon guidance across the CNS/PNS transition zone. Dev Biol 238:47–63. CrossRef Medline

Stork T, Engelen D, Krudewig A, Silies M, Bainton RJ, Klämbt C (2008) Organization and function of the blood–brain barrier in *Drosophila*. J Neurosci 28:587–597. CrossRef Medline

Sun B, Xu P, Salvaterra PM (1999) Dynamic visualization of nervous system in live Drosophila. Proc Natl Acad Sci U S A 96:10438–10443. CrossRef Medline

Swierczek NA, Giles AC, Rankin CH, Kerr RA (2011) High-throughput behavioral analysis in C. elegans. Nat Methods 8:592–598. CrossRef Medline

Tsai PI, Wang M, Kao HH, Cheng YJ, Lin YJ, Chen RH, Chien CT (2012) Activity-dependent retrograde laminin A signaling regulates synapse growth at Drosophila neuromuscular junctions. Proc Natl Acad Sci U S A 109:17699–17704. CrossRef Medline

Urbano JM, Torgler CN, Molnar C, Tepass U, López-Varea A, Brown NH, de Celis JF, Martín-Bermudo MD (2009) Drosophila laminins act as key regulators of basement membrane assembly and morphogenesis. Development 136:4165–4176. CrossRef Medline

von Hilchen CM, Bustos AE, Giangrande A, Technau GM, Altenhein B (2013) Predetermined embryonic glial cells form the distinct glial sheaths of the Drosophila peripheral nervous system. Development 140:3657–3668. CrossRef Medline

Wallquist W, Plantman S, Thams S, Thyboll J, Kortesmaa J, Lännergren J, Domogatskaya A, Ogren SO, Risling M, Hammarberg H, Tryggvason K, Cullheim S (2005) Impeded interaction between Schwann cells and axons in the absence of laminin alpha4. J Neurosci 25:3692–3700. CrossRef Medline

Wilson DG, Phamluong K, Li L, Sun M, Cao TC, Liu PS, Modrusan Z, Sandoval WN, Rangell L, Carano RA, Peterson AS, Solloway MJ (2011) Global defects in collagen secretion in a Mia3/TANGO1 knockout mouse. J Cell Biol 193:935–951. CrossRef Medline

Wolfstetter G, Holz A (2012) The role of LamininB2 (LanB2) during mesoderm differentiation in Drosophila. Cell Mol Life Sci 69:267–282. CrossRef Medline

Xie X, Auld VJ (2011) Integrins are necessary for the development and maintenance of the glial layers in the Drosophila peripheral nerve. Development 138:3813–3822. CrossRef Medline

Yang D, Bierman J, Tarumi YS, Zhong YP, Rangwala R, Proctor TM, Miyagoe-Suzuki Y, Takeda S, Miner JH, Sherman LS, Gold BG, Patton BL (2005) Coordinate control of axon defasciculation and myelination by laminin-2 and -8. J Cell Biol 168:655–666. CrossRef Medline

Yu WM, Feltri ML, Wrabetz L, Strickland S, Chen ZL (2005) Schwann cell-specific ablation of laminin γ1 causes apoptosis and prevents proliferation. J Neurosci 25:4463–4472. CrossRef Medline

Yu WM, Yu H, Chen ZL (2007) Laminins in peripheral nerve development and muscular dystrophy. Mol Neurobiol 35:288–297. CrossRef Medline

Yu WM, Chen ZL, North AJ, Strickland S (2009a) Laminin is required for Schwann cell morphogenesis. J Cell Sci 122:929–936. CrossRef Medline

Yu WM, Yu H, Chen ZL, Strickland S (2009b) Disruption of laminin in the peripheral nervous system impedes nonmyelinating Schwann cell development and impairs nociceptive sensory function. Glia 57:850–859. CrossRef Medline

Yurchenco PD (2011) Basement membranes: cell scaffoldings and signaling platforms. Cold Spring Harb Perspect Biol 3:pii:a004911. CrossRef Medline

Yurchenco PD, Quan Y, Colognato H, Mathus T, Harrison D, Yamada Y, O'Rear JJ (1997) The α chain of laminin-1 is independently secreted and drives secretion of its β- and γ-chain partners. Proc Natl Acad Sci U S A 94:10189–10194. CrossRef Medline